Investigation of the thermal degradation of PET, zinc phosphinate, OMPOSS and their blends—Identification of the formed species

Aurore Vannier[a], Sophie Duquesne[b,*], Serge Bourbigot[b], Jenny Alongi[c], Giovanni Camino[c], René Delobel[a]

[a] Centre de Recherche et d'Etude sur les Procédés d'Ignifugation des Matériaux (CREPIM), Parc de la porte Nord, F-62200 Bruay-la-Buissière, France
[b] Laboratoire des Procédés d'Elaboration de Revêtements Fonctionnels (PERF), UMR-CNRS 8008/LSPES – Ecole Nationale Supérieure de Chimie de Lille, BP 90108, F-59652 Villeneuve d'Ascq, France
[c] Centro di Cultura per l'Ingegneria delle Materie Plastiche – Politechnico di Torino, V.le T. Michel, 5, 15100 Alessandria, Italy

ARTICLE INFO

ABSTRACT

The incorporation of both OMPOSS and Exolit OP950 (zinc phosphinate) into PET leads to increased fire retarding properties and a synergistic effect has been established between the three components. Here the thermal degradation of OMPOSS, Exolit OP950, PET and blends of them is investigated via thermal degradation in pyrolytic and thermo-oxidative conditions. All species formed during the degradation of the additives or the blends are identified by solid state NMR and X-ray diffraction in the condensed phase and by GC–MS in the gas phase. The investigation shows that no chemical interaction occurs between the additives, which suggests that the synergy responsible for the improvement of fire properties of the material has a physical origin.

1. Introduction

The large variety of polyhedral oligomeric silsesquioxane (POSS) allows their application in multiple fields. They are usually used as mechanical reinforcement in polymers. Devaux [1], Bourbigot [2] and Fina [3] used different POSS alone to get a better fire behaviour of polymers. The use of POSS as synergist in fire retarded polymers, has only been studied by Chigwada [4] and in our Laboratory. Chigwada incorporated vinyl POSS and tricresylphosphate into poly(vinylester) and obtained a reduction of 68% of the peak of heat released (pHRR) (with 5% of vinyl POSS and 30% of tricresylphosphate). In our Lab a synergistic effect has been highlighted between octa methyl POSS (OMPOSS) and a zinc phosphinate (OP950) that lead to a high improvement of the fire properties of the PET [5]. Indeed, whereas the incorporation of 10% of OP950 into polyethylene terephtalate (PET) lead to a decrease of the pHRR (−37%) and an increase in the limiting of oxygen index (LOI) value (+3 vol.%), the substitution of only 1% of OP950 with OMPOSS brings those results to −61% for the pHRR decrease and +10 vol.% for the LOI. This synergistic effect can be due to physical interactions or chem-

ical interactions between the components of the formulation. In this paper, we propose to investigate the eventual chemical interactions that might occur between the additives in the first step and between the additives and the polymer in a second step.

To highlight chemical interactions occurring during the combustion of the different components, a systematic approach is used. Each component and blend undergoes a thermal treatment in an oven at different characteristic temperature chosen from the TGA of the components. The residues of the thermal treatments are then analysed by solid state NMR and X-ray diffraction. To complete the obtained information, the different additives also undergo a pyrolysis and the gases evolved from those pyrolysis are analysed by gas chromatography coupled with a mass spectrometer.

2. Experimental

2.1. Materials

The following products were used.

PET is a mixture between 15 wt.% of virgin PET pellets and 85 wt.% of recycled flakes, supplied by Wellman Company. Exolit OP950 is a phosphinated compound of general formula $[R_1R_2POO]_n{}^- M^{n+}$, where R_1 and R_2 are ethyl groups and the metal ion is Zn^{2+} ion, kindly provided by Clariant. Octa methyl polyhedral
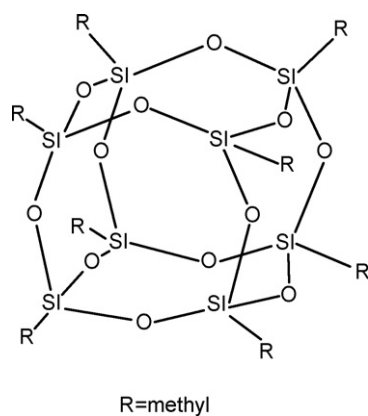
R=methyl

Fig. 1. Structure of OMPOSS.

oligomeric silsesquioxane (OMPOSS) was purchased from Hybrid Plastics Company and used as received (Fig. 1).

2.2. Processing

Materials were mixed under nitrogen at 275 °C using a Brabender mixer (type 350/EH, roller blade, mixing conditions checked using the data processing torque rheometer system PL2000, constant shear rate: 50 rpm).

2.3. Thermo-oxidative degradation

In order to simulate the degradation process of the different additives and their blends, thermal treatments have been carried out in a tubular furnace under air. Samples of approximately 1 g (in powder for the additives and in bulk for the polymeric materials) have been treated for 3 h at temperatures characteristic of the different steps of degradation based on TG curves (300, 400 and 500 °C). The samples are directly introduced into the furnace, without any ramp. Residues are analysed with X-ray diffraction and solid state NMR.

Analysed samples were: OP950, OMPOSS, mix OP950 90%–OMPOSS 10%, PET, PET–OP950 10%, PET–OP950 9%–OMPOSS 1%.

2.4. Thermal volatilisation analysis (pyrolysis)

TVA analysis has been used to identify the gases evolved during the degradation under nitrogen of the samples. Samples of around 1 g were placed in a vertical oven and underwent a temperature ramp from 20 to 500 °C and an isotherm at 500 °C for 2 h. The gases evolved during the pyrolysis are trapped into two traps: one at −80 °C (ethanol + liquid nitrogen) and another one at −196 °C (liquid nitrogen). Once at ambient temperature, the gases were analysed by gas chromatography coupled to a mass spectrometer (GC–MS). Residues are also analysed by solid state NMR.

Analysed samples were: OP950, OMPOSS.

2.5. Analysing tools

2.5.1. X-ray diffraction

XRD spectra were recorded in the 5–60° 2θ-range using a Brucker AXS D8 diffractometer ($\lambda_{(Cu\ K\alpha)}$ = 1.5418 Å, 40 keV, 25 mA) in configuration $2\theta/\theta$. The acquisition parameters were as follows: step of 0.02°, step time of 2 s. The data are analysed using the diffraction patterns of Inorganic Crystal Structure Database (ICSD).
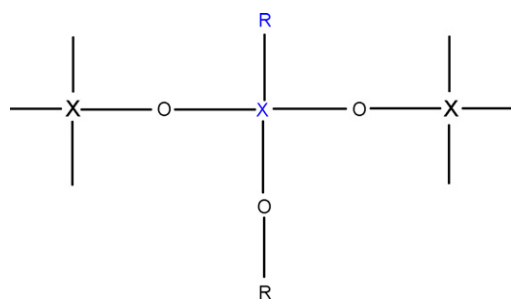

Fig. 2. Example of the nomenclature M, D, T, Q with an atom X T^2.

2.5.2. Solid state NMR

NMR measurements were performed on a Bruker Avance II spectrometer (2.35 T and 9.4 T) using 4 or 7 mm probes and magic angle spinning (MAS). ^{13}C NMR measurements were performed at 25.2 MHz with ^{1}H–^{13}C cross-polarisation (CP). For all samples, a repetition time of 5–10 s, a contact time of 1 ms and a spinning speed of 5 kHz were used. The reference used was the tetramethylsilane (TMS)

^{31}P NMR measurements were performed at 40.5 MHz with and without ^{1}H–^{31}P CP (contact time of 2 ms) and with dipolar decoupling. Experiments without CP were performed with a repetition time varying from 5 to 60 s according to the relatively long relaxation time of phosphorous compounds. With CP, the repetition time is fixed at 5 s as the relaxation time of protons is shorter. Spectra acquired were the result of the accumulation of 8–64 scans without CP and 8–256 scans with CP. The reference used was 85% H_3PO_4 in aqueous solution.

^{29}Si measurements were performed at 19.6 MHz with and without ^{1}H–^{29}Si CP and dipolar decoupling with a MAS speed of 4 kHz. The repetition time applied was varying between 5 and 10 s and the contact time fixed at 8 ms. TMS is used as a reference.

The X atom can be designated by the letter M, D, T, Q based on the nature of its surrounding: 3, 2, 1 or no R (alkyl) group (and thus 1, 2, 3 or 4 –O– bond). To this letter is added a superscripted number referring to the number of –O–X bond linked to the X atom concerned. An example of this nomenclature is given in Fig. 2.

2.5.3. GC–MS

Volatile species have been analysed with a Perkin Elmer Turbomass Gold mass spectrometer (ionisation energy 70 eV) coupled to a Perkin Elmer Autosystem XL gas chromatographer with a capillary column VF-1 (length 30 m, diameter 0,25 mm, thickness 1 μm). The vector gas was helium (1 mL min^{-1}), the temperature of the injection chamber was fixed to 280 °C and the temperature ramp applied was 10 °C min^{-1} between 50 and 300 °C. The identification of the different substances is realised through the analyses of the fragments masses of the substances validated by comparison with the NIST Chemistry Book Database [6].
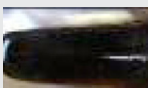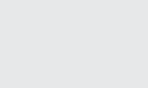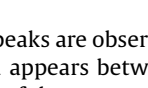
3. Results

3.1. Degradation of OP950

3.1.1. Thermo-oxidative degradation

According to our previous work [5], OP950 degrades in two steps under air, the first one between 268 and 432 °C (maximum degradation rate 417 °C) and the second one between 432 and 694 °C (maximum degradation rate 486 °C). The photos of the residues of the different species studied after the different thermal treatments are presented in Table 1. After 300 and 400 °C thermal treatments, OP950 has melt and is solidified. After the 500 °C treatment, OP950 has swelled and carbonised. Intumescence has appeared.

Table 1
Photos of residues of the degradation of the samples under air.

Temperature	300 °C	400 °C	500 °C
OP950			
OMPOSS			
OP950–OMPOSS			
PET–OP950			
PET–OP950–OMPOSS			

In Fig. 3 are presented the NMR CP MAS ^{13}C spectra of OP950 and of its residues at different thermal treatments. For non-treated OP950, a peak at $\delta_c = 6.5$ ppm and a doublet at $\delta_c = 20$ and 24 ppm are observed. The peak at 6.5 ppm is representative of the two methyl groups of the phosphinates that are chemically equivalent. The doublet at 20 and 24 ppm represents unshielded C belonging to $-CH_2-$ groups linked to the phosphorous atom. After 300 and 400 °C thermal treatments, peaks are broader but the same species are identified. This enlargement could be attributed to a partial loss of crystallinity of the component. After a 500 °C thermal treatment, a broad peak appears at $\delta_c = 123$ ppm, characterising aromatic carbons of the char. A broad band is now observed in the aliphatic region (region of the carbon of the phosphinates). The chemical shifts are slightly shifted that means that the molecule has changed. Aliphatic carbons remain the same than those of the phosphinates (CH_3–CH_2–P bonds) but the phosphorous is no longer in the phosphinate configuration but in a phosphonate or a phosphate configuration as shown by ^{31}P NMR (see comments below).

Fig. 4 represents NMR ^{31}P CP-DD-MAS and DD-MAS spectra of OP950 and of its residues after different thermal treatments. Four peaks appear at $\delta_P = 45$, 47, 52 and 53 ppm for the non-treated OP950. They represent the D^0 phosphorous in the phosphinate molecule. The presence of 4 different peaks can be attributed to different crystallographic configurations of the phosphorous in the phosphinate. After a 300 °C thermal treatment, peaks are observed with the same chemical shift but a broad band appears between $\delta_P = 45$ and 53 ppm. A partial loss of crystallinity of the component during the thermal treatment and thus the presence of an amorphous component can explain the enlargement of the peak between 45 and 53 ppm and the conservation of the original peaks of the non-treated phosphinate. Same peaks are observed after a 400 °C thermal treatment. The large band between 45 and 53 ppm is less visible but is still there as the baseline does not go back to zero. After a 500 °C thermal treatment, bands relative to the phosphorous in the phosphinate have disappeared but three broad bands, centred at $\delta_P = 23$, -8 and -27 ppm appear as well as a small peak at $\delta_P = -2$ ppm. These chemical shifts are respectively attributed to the presence of phosphonates (phosphorous T^0), pyrophosphates (phosphorous Q^1), ramified polyphosphates (phosphorous Q^3) and phosphates (phosphorous Q^0). Because of the aliphatic carbons detected by ^{13}C NMR, it is reasonable to assume that the phosphonates formed are ethylphosphonates. Those bands are also detectable after the 400 °C thermal treatment but with a very low intensity (cf. framed graph of the 400 °C thermal treatment). This shows that they are formed from the second step of degradation of the phosphinate.

Fig. 5 represents diffractograms of non-treated OP950 and of the residues of its degradations at 300, 400 and 500 °C. At ambient temperature and after the 300 and 400 °C thermal treatments, OP950 keeps certain crystallinity. After the 500 °C thermal treat-
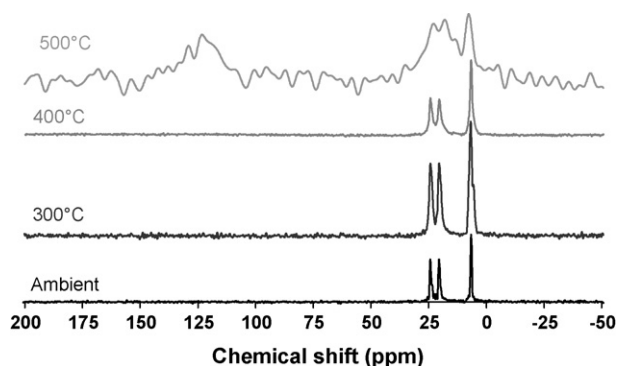

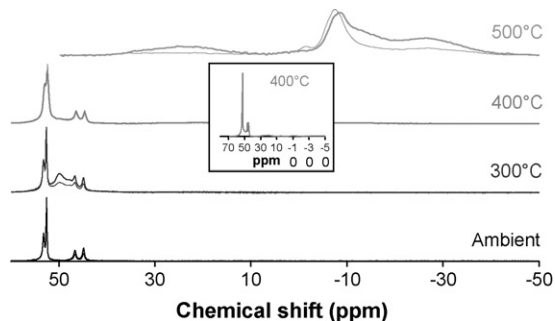**Fig. 3.** NMR CP MAS ^{13}C spectra of OP950 and of the residues of its thermal treatments.

Fig. 4. NMR ^{31}P spectra of OP950 and of the residues of its thermal treatments (CD DD MAS thick curves and DD MAS thin curves).
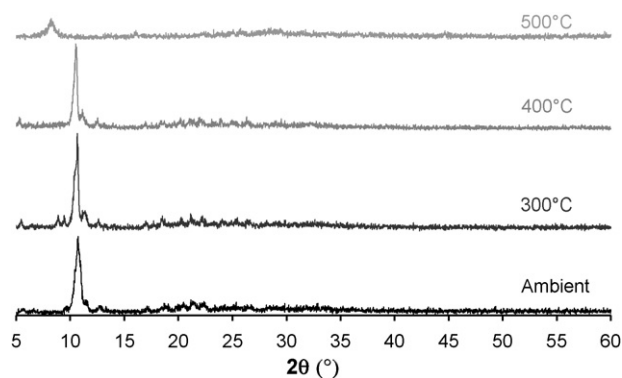
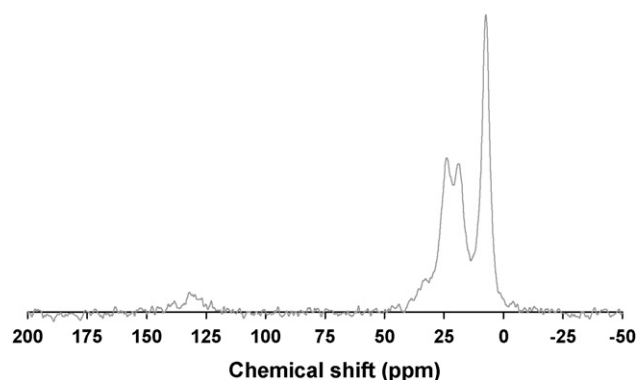**Fig. 5.** XRD spectra of OP950 and of the residues of its thermal treatments.

Fig. 7. NMR ^{31}P spectrum of the residues of OP950 after the TVA experiment with (thick curve) and without (thin curve) CP (*rotation bands).

The phosphate peak at $\delta_P = 2$ ppm had a low intensity during the degradation under air and appears more neatly here. Whereas the atmosphere is inert, oxidised species are still formed. This suggests that the oxidation of phosphinate is not only due to the oxygen of the air but also via intermolecular reactions. Oxygen atoms of the phosphinates allow to oxidise a part of the phosphinates into phosphonates and then into phosphates. Under nitrogen, non-oxidised phosphinates remain. The time of the experiment, shorter during the TVA than during the thermo-oxidative experiment, could explain the incomplete conversion of the phosphinates into phosphonates and phosphates (kinetic effect). On the other hand, it is noteworthy that in the absence of CP, the peak of the phosphonates of the pyrolysis residues ($\delta_P = 25$ ppm) is 16 times more important in the case of the thermo-oxidative degradation. It suggests that, without the oxygen contained in air, a smaller quantity of the formed phosphonates is oxidised into phosphates or pyrophosphates rather than polyphosphates (the intensity of the -27 ppm band is lower than in the case of the thermo-oxidative degradation). However, those species are still formed at this temperature and their presence is not dependant of the nature of the atmosphere. Oxygen contained in air catalyses the degradation of phosphinates but their oxidation also happens via intermolecular reactions and not only with the oxygen of air.

Fig. 6. NMR ^{13}C spectrum of the residues of OP950 after the TVA experiment.

ment, OP950 is degraded. Its degradation leads to the formation of a poorly crystallised specie with a peak at $2\theta = 8.3°$. This unique peak suggests the presence of zinc dipyrophosphate $Zn_4(P_2O_7)_2$ [7] which is consistent with what has been observed with solid state NMR.

3.1.2. Pyrolysis

Figs. 6 and 7 show ^{13}C and ^{31}P (with and without CP) NMR spectra of the residues of OP950 after the TVA analyses.

On ^{13}C NMR spectra, the peaks present are the same than those present after the degradation in air:aliphatic carbons between $\delta_C = 0$ and 50 ppm and carbons of the char around 130 ppm, which intensities are lower than those of the aliphatic carbons.

As for the degradation under air, on ^{31}P NMR spectra, peaks at $\delta_P = 23$ and -9 ppm are detected. They evidence the presence of phosphonates and pyrophosphates in the residue. The peak of the phosphinate is still present but the band is broad which could be explained as suggested above by a loss in the crystallinity of OP950.
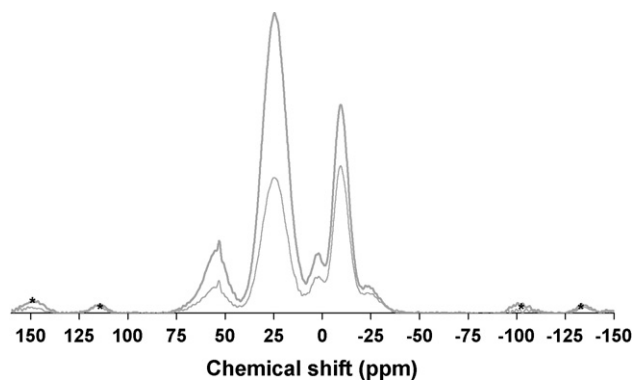
3.1.3. Gas phase analysis

Chromatograms of the gases obtained during the degradation of OP950 under nitrogen are presented in Fig. 8. The different components have been separated by chromatography. First peaks at 1.00 and 1.46 (time unit) correspond to water and acetone coming from the cleaning of the apparatus. However, the chromatogram of the gases coming from the trap at $-80°C$ reveals the presence of a peak having a very low intensity at 3.21. The mass spectrum of this component is presented in Fig. 9. The analysis of this spectrum reveals
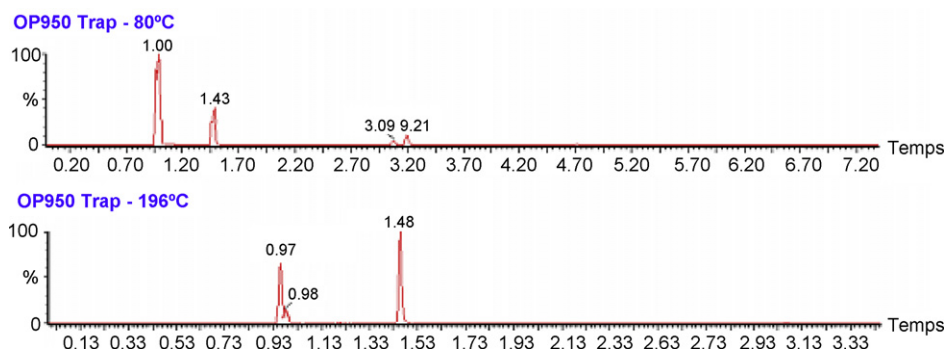

Fig. 8. Chromatograms of the gases evolved during the degradation of OP950 under nitrogen in the different traps.
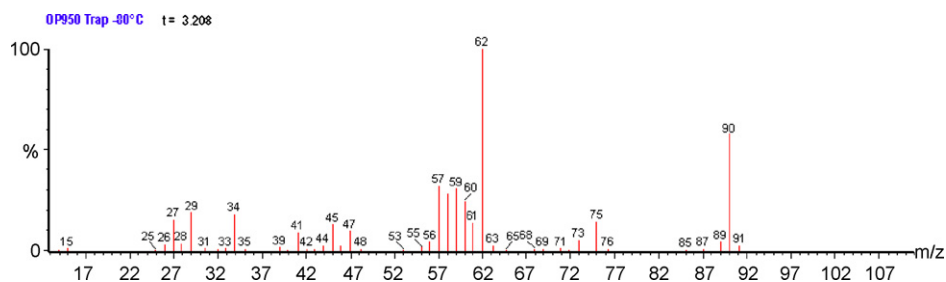
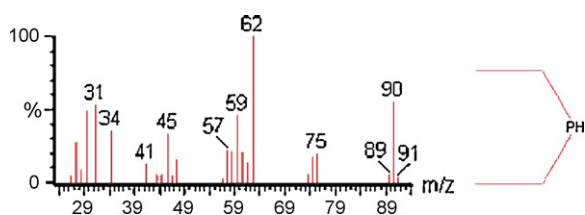**Fig. 9.** Mass spectrum of phosphine coming from the degradation of OP950 under nitrogen.

Fig. 10. Spectrum and structure of the diethyl phosphine.

the presence of diethyl phosphine (mass spectrum presented in Fig. 10).

The presence of reduced species reinforces the hypothesis that oxygen of the phosphinates allows their oxidation into phosphonates. A dismutation occurs within the phosphinate molecule leading to the formation of an oxidised species, the phosphonate on the one hand, and into reduced specie, the phosphine on the other hand.

3.2. Degradation of OMPOSS

3.2.1. Thermo-oxidative degradation

According to our previous work [5], OMPOSS degrades in a main step followed with a small degradation of the remaining residue. This step occurs between 207 and 305 °C with a mass loss of 95%. Fina [8] showed that POSS cages break and lead to the formation of amorphous silica. The behaviour of the POSS is different from the one of the other components. It decomposes directly to gas products. It is also possible that it sublimates and recondenses into the tube in the oven. Particles are carried away and barely any residue remains after 300 °C in TGA. However, after a 300 or 500 °C thermal treatment, a crust is formed at the surface that prevents the underneath product to volatilise as it happens during a slow ramp of temperature (conditions of the TGA). The photos of the residues of OMPOSS after the different thermal treatments are shown in Table 1. A white powder (presumably silica) is formed at high temperature.

In Fig. 11 are shown the ^{13}C NMR CP MAS spectra of OMPOSS and of the residues of its thermal treatments. At ambient temperature, a unique peak is observed at $\delta_C = -5$ ppm, assigned to alkyl groups (CH$_3$) linked to silicon atoms. At 300 and 400 °C, Si–CH$_3$ bonds are still there. However, the peak is broader. This phenomenon can be explained by the loss of crystallinity of the POSS as it is demonstrated in Fig. 12 according to the diffractogrammes of OMPOSS after the different thermal treatments. Indeed, after 300 and 500 °C thermal treatments, no signal is detected by X-ray diffraction, showing the amorphous property of the residues. Moreover, at high temperature, bonds of OMPOSS (Si–C; Si–O) break to form a large number of fragments whose chemical shifts are similar than those of the original POSS that lead to a widening of the peak. After the 500 °C thermal treatment, the detection of the species is more difficult which can be caused by a low concentration in Si–C bonds and by a distortion of cages.
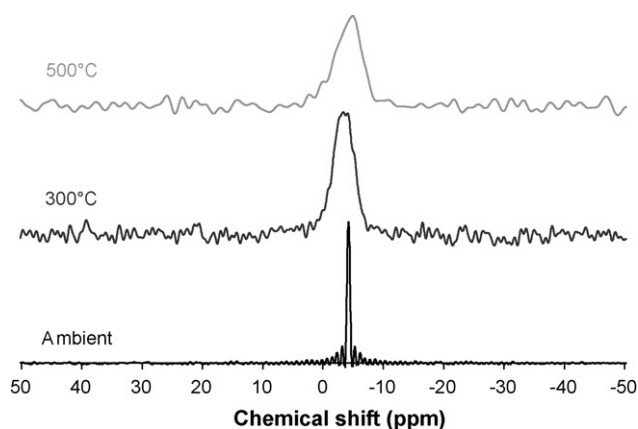

Fig. 11. NMR CP MAS ^{13}C spectra of OMPOSS and of the residues of its thermal treatments.
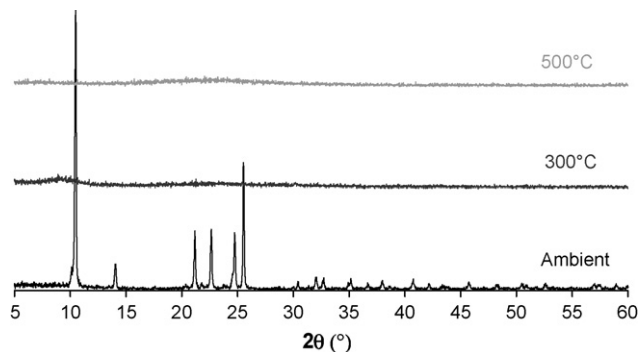

Fig. 12. Diffractograms of OMPOSS and of the residues of its degradation.

Fig. 13 represents ^{29}Si NMR of the same samples with and without CP. At ambient temperature, two peaks at $\delta_{Si} = -66$ and -66.7 ppm are assigned to Si atoms in the T^3 configuration that is to say linked to a CH$_3$ group and to 3 –O–Si groups. After a
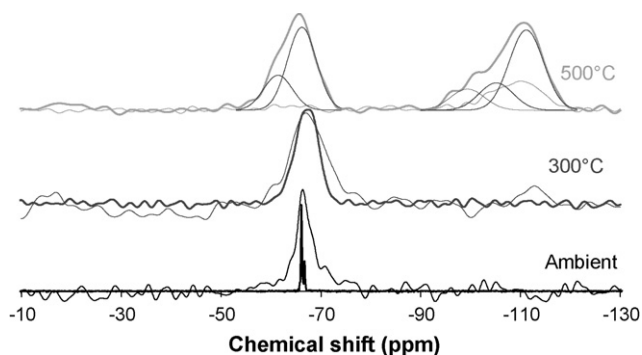

Fig. 13. NMR CP MAS ^{29}Si spectra of OMPOSS and of the residues of its thermal treatments (CP DD MAS thick curves, DD MAS thin curves).
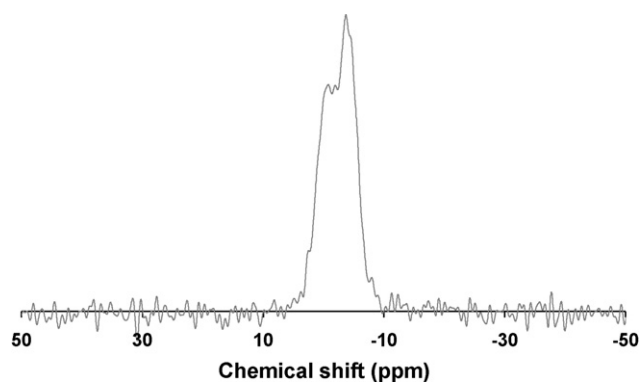
Fig. 14. ^{13}C NMR spectrum of the residues of OMPOSS after the TVA.

Fig. 15. ^{29}Si NMR CP MAS spectrum of the residues of OMPOSS after the TVA.

300 °C thermal treatment, the peak becomes broader but has the same chemical shift. After the 500 °C thermal treatment, two large bands are visible with CP. The first one exhibiting 3 peaks (after deconvolution) at $\delta_{Si} = -98, -104$ and -110 ppm assigned to Q^2, Q^3 and Q^4 silicon atoms [9] linked respectively to two, three or four O–Si groups which represent a silica network. Without CP the signals of Q^2 and Q^3 silicon are weaker and difficult to distinguish. This confirms the presence of hydroxyl final groups of silica of Q^2 and Q^3 silicon [–(SiO)$_2$–Si–(OH)$_2$] and [–(SiO)$_3$–Si–(OH)] that permit to enhance the signal of those bands that would be lost in the background noise otherwise. The second band, remaining at $\delta_{Si} = -66$ ppm (T^3 Si) corroborates what has been observed in ^{13}C NMR, that is to say Si–C bonds. However, this bond is not present without CP. If we assume that CP is efficient in our experimental conditions, it means that the quantity of T^3 Si in the residue is very low and that their detection is difficult because of the non-enhancing effect of CP. Thus, during its degradation, OMPOSS degrades into a silica network while conserving Si–CH$_3$ ending groups that were present in the initial cages.

3.2.2. Pyrolysis

The ^{13}C NMR analysis of the residues of OMPOSS after the TVA is presented in Fig. 14. A broad band is distinguishable between $\delta_C = 0$ and -10 ppm as for the degradation in air, so it is possible to draw the same conclusions, that is to say the presence of Si–C bonds and fragments that have close chemical shifts. Fig. 15 represents the [29]Si spectrum of the residues of OMPOSS after the TVA. Same bands are present as for the residues of the degradation under air at 500 °C (Q^4, Q^3, Q^2 Si at $\delta_{Si} = -110$ ppm and T^3 Si at $\delta_{Si} = -66$ ppm). However, an additional peak appears at $\delta_{Si} = -20$ ppm. This chemical shift is characteristic of D^2 Si (–R$_2$–Si–(OSi)$_2$). During the degradation, OMPOSS rearranges to form a silica network which terminal groups contain one or two methyl groups. It is possible to suppose that under air, these D^2 Si, which are not present in the residue, are oxidised and lead to the formation of Si of type Q or T.

3.2.3. Gas phase analysis

The chromatogram obtained for the gases evolved during pyrolysis of OMPOSS at 500 °C is presented in Fig. 16. Pollutants such as acetone or acetaldehyde are present in the bigger peaks of the
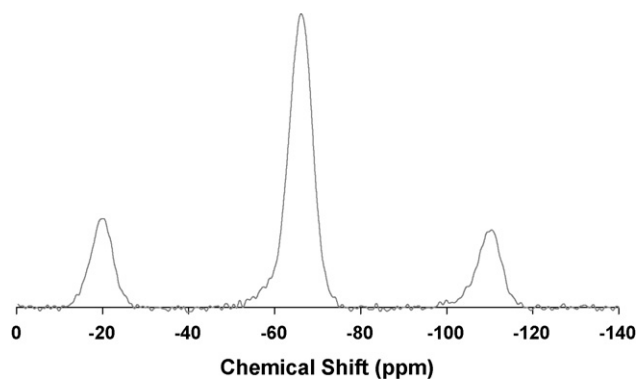
chromatogram but their probability to come from OMPOSS is very low. However, at 1.99 and 3.41 (time unit) the mass spectra (Fig. 17) reveal the presence of siliconorganic species that can be attributed respectively to trimethylsilanol (M^0 Si) or hexamethyldisiloxane (M^1 Si) whose chemical formula and mass spectra are presented in Fig. 18. (NB: The trimethyl silanol can result from the hydrolysis of hexamethyl disiloxane.)

In the gas phase, reduced siliconorganic species compared to the one in the condensed phase are found. During the pyrolysis, a part of the T^3 silicon of the OMPOSS is reduced into M^1 or M^0 Si, whereas another part is oxidised into Q^2, Q^3 or Q^4 Si.

3.3. Degradation of OMPOSS–OP950

3.3.1. Thermo-oxidative degradation

In order to study the eventual chemical interactions between OP950 and OMPOSS, those two additives have been mixed in the proportions 90/10 (we remind the reader it is at this ratio that the highest synergistic effect in terms of flame retardancy is obtained [5]). In Table 1, it is observed that the residues of the thermal treatment of the mix at 300 and 500 °C are similar to the residues of the thermal treatment of OP950. That is to say, at 300 °C, the OP950 has melt and has solidified while going back to room temperature. At 500 °C, the mix has intumesced leading to an expanded carbonaceous product. At 400 °C however, whereas OP950 was only melted, its mixture with OP950 has intumesced to form a black crust on the top and a white rigid mousse residue inside.

In Figs. 19–21 are presented respectively the ^{13}C CP MAS, the [29]Si CP MAS and the ^{31}P CP MAS and MAS NMR spectra of the mix OP950–OMPOSS and of its residues after the different thermal treatments. The spectra, whatever the temperature of thermal treatment, consist in the superposition of the spectra of OP950 and OMPOSS taken separately. In ^{13}C NMR the peaks of the aliphatic carbons are found between $\delta_c = -10$ and 25 ppm. After a 400 °C thermal treatment, the peak relative to the carbons of OMPOSS is less detectable but after the 500 °C thermal treatment, all the peaks are found which show that the peaks of the phosphinate have their intensity lowered. The formation of condensed aromatic carbons after the 500 °C thermal treatment is visible because of the peak at $\delta_c = 130$ ppm assigned to aromatic carbons.

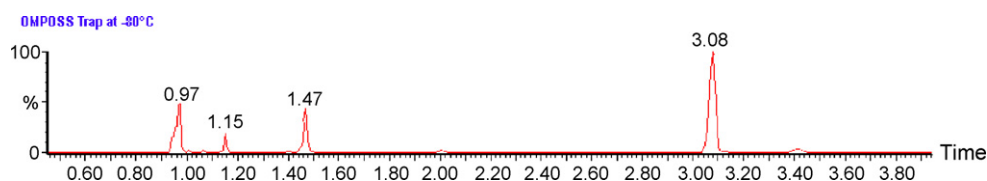**Fig. 16.** Chromatogram of the gases evolved from the pyrolysis of OMPOSS at 500 °C in the trap at −80 °C.
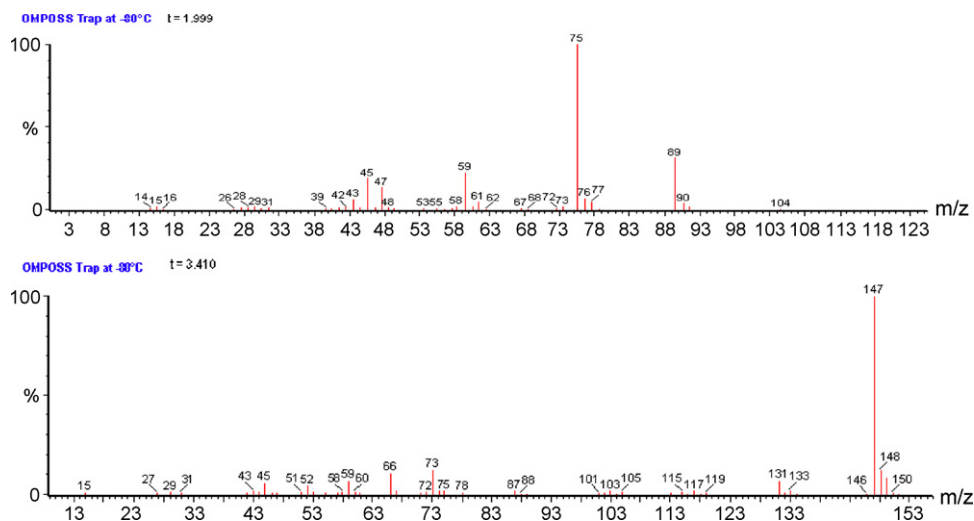
Fig. 17. Mass spectra of the products coming from the pyrolysis of OMPOSS at 500 °C.
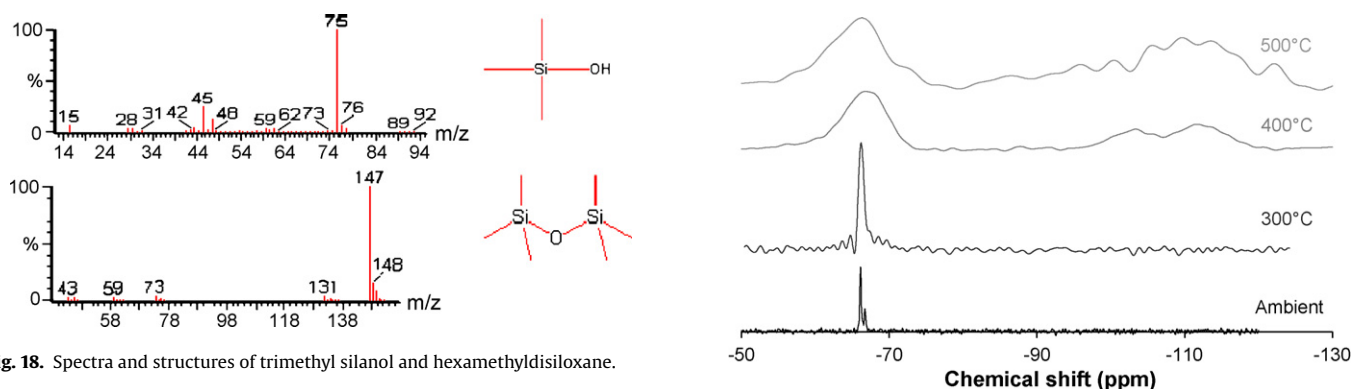

Fig. 18. Spectra and structures of trimethyl silanol and hexamethyldisiloxane.

Fig. 20. ^{29}Si CP MAS NMR spectra of the mix OP950–OMPOSS and of the residues of its thermal treatments.

In ^{29}Si NMR, peaks corresponding to T^3 silicon (-66 ppm) are detected as shown in the previous section as well as the peaks attributed to Q^3 and Q^4 silicons of the silica network ($\delta_{Si} = -103$ and -110 ppm) from the 400 °C thermal treatment. The resolution of these last peaks is nevertheless lower than for OMPOSS treated alone. The formation of amorphous silica leads to the enlargement of the peak. Moreover, we established that OMPOSS was decomposing to gas products and/or sublimating and according to the few quantity of OMPOSS in the mix at the beginning (10%), the loss of material explains the loss of the signal.

In ^{31}P NMR, peaks that were observed for OP950 alone are also detected here. Peaks relative to phosphinates at $\delta_P = 45, 47, 52$ and

53 ppm are observed at ambient temperature. The presence of an amorphous phase and thus of a broad band centred at 50 ppm at 300 and 400 °C is highlighted. Finally, peaks attributed to phosphonates ($\delta_P = 24$ ppm), phosphates ($\delta_P = -2$ ppm) and pyrophosphates ($\delta_P = -10$ ppm) are visible after the 500 °C thermal treatment and detectable from the 400 °C thermal treatment.

No additional species is formed during the simultaneous degradation of OP950 and OMPOSS. Those two components do not react one with the other. That is why the TVA analysis has not been performed on the mix.
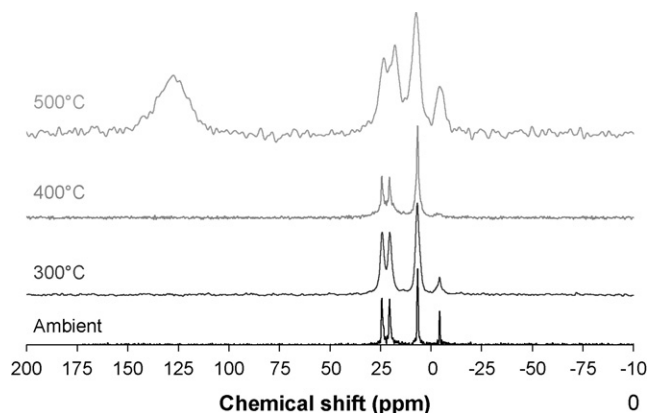

Fig. 19. ^{13}C CP MAS NMR spectra of the mix OP950–OMPOSS and of the residues of the mix after thermal treatments.
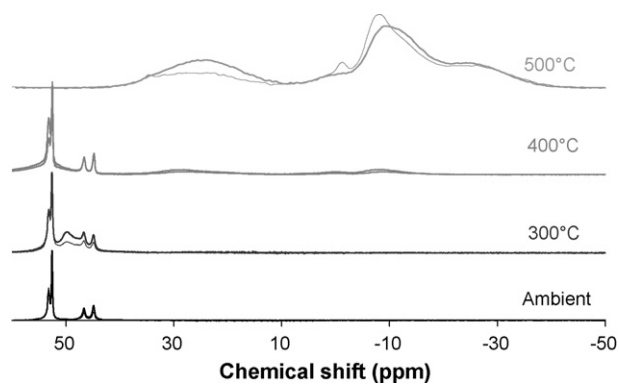

Fig. 21. ^{31}P DD NMR spectra of the mix OP950–OMPOSS and of the residues of its thermal treatments (CP MAS thick curves and MAS thin curves).
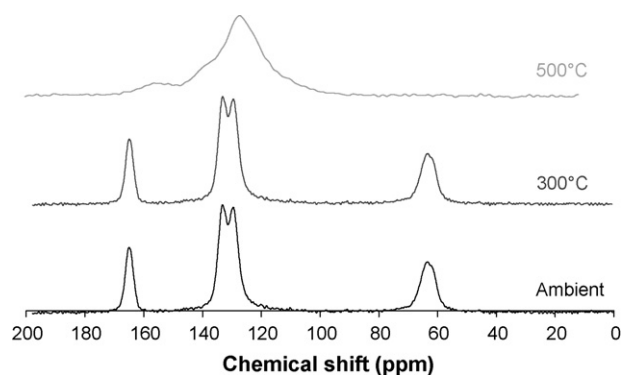
Fig. 22. CP MAS ^{13}C NMR spectra of PET and of the residues of its thermal treatments.

3.4. Degradation of PET

3.4.1. Thermo-oxidative degradation

Fig. 22 shows ^{13}C NMR CP MAS spectra of PET and of the residues of its thermal treatments. For spectra of non-treated PET and of PET treated at 300 °C, the chemical shifts observed are those listed in the literature: a peak at $\delta_C = 61$ ppm is assigned to alkyls groups ($-CH_2-CH_2-$), a band between $\delta_C = 129$ and 133 ppm is assigned to aromatic groups (benzenic cycles) and a peak at $\delta_C = 165$ ppm is due to C=O bond of the PET. After the treatment at 500 °C, PET is degraded. Peaks attributed to aliphatic carbons and those attributed to C=O bonds of the PET disappeared to give a broad band between $\delta_C = 156$ and 127 ppm that is due to the formation of carbonyl groups and condensed aromatic compound that are present in the char.

The gas phase analysis (not presented here) shows the presence of acetaldehyde, furan, benzene, toluene, p-xylene, 1,3-dioxolan and para-aldehyde. All these species have been previously listed in the literature [10,11].

3.5. Degradation of PET–OP950

The gases evolved during the pyrolysis of the formulations PET–OP950 and PET–OP950–OMPOSS do not reveal the presence of phosphorous or siliconorganic species. Indeed, the concentrations of OP950 and OMPOSS are low in the polymer and the phosphorous or siliconorganic gases, if they are evolved, cannot be detected because of their low concentration compared to the concentrations of the gases released by PET. That is why only the analysis of the condensed phase is presented in the following of the study.

3.5.1. Thermo-oxidative degradation

The pictures of the residues of the degradation of the formulation PET–OP950 show that, at 300 °C, the polymer and the phosphinate have molten. The residue is black and is solidified as it went back to ambient temperature. After a 400 °C thermal treatment, an alveolar structure showing large cells is formed. Intumescence is observed. At this temperature, OP950 alone melts whereas it swelled with OMPOSS. Here, as PET is a char former polymer, it seems that it intumesced.

Figs. 23 and 24 show respectively the ^{13}C NMR CP MAS spectra and the ^{31}P MAS spectra of the blend PET–OP950 at ambient temperature and treated at 300, 400 and 500 °C. Spectra of the non-treated blend and of the blend treated at 300 °C consist in the superposition of the spectra of PET and OP950 taken separately.

In ^{13}C NMR, the chemical shifts of aliphatic carbons of PET and OP950 are found at $\delta_C = 6.5$; 20.5; 24 and 61 ppm. The chemical shifts of aromatic carbons are observed between $\delta_C = 129$ and 133 ppm and of carbonyls at $\delta_C = 163$ ppm for the non-treated blend and the blend treated at 300 °C. From 400 °C, PET degrades and
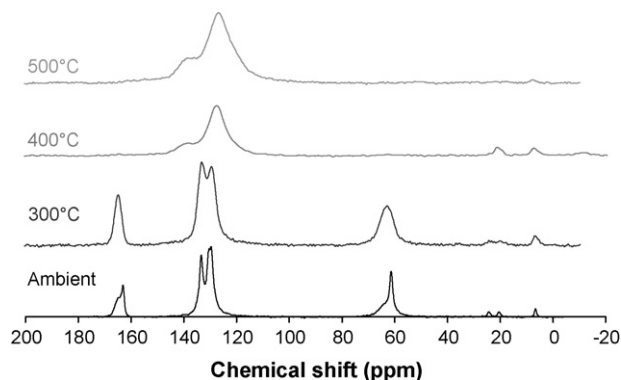

Fig. 23. CP MAS ^{13}C NMR spectra of the blend PET–OP950 10% and of its residues of thermal treatments.

peaks of condensed carbonaceous structure appear at $\delta_C = 123$ ppm whereas the peaks of the aliphatic carbons of the phosphinates remain at $\delta_C = 7$ and 20 ppm. After the 500 °C thermal treatment, the same chemical shifts are observed. However, as for the thermal treatment of OP950 alone, the intensity of the carbons of the phosphinates have lowered and almost lost in the background.

In ^{31}P NMR, the chemical shifts of the phosphinates at ambient temperature are found (around $\delta_P = 50$ ppm). After the 300 °C thermal treatment, the chemical shift observed does not change (centred at $\delta_P = 50$ ppm) but the peak is considerably enlarged. With the simultaneous melting of OP950 and PET, it is possible to assume that this enlargement is due to the loss of crystallinity of the system or to the superimposition of the peaks of crystallised and amorphous species.

Thermal treated alone or with OMPOSS, phosphinate does not degrade until 400 °C. Whereas introduced into PET, its degradation appears at lower temperature. Indeed, from 400 °C, a broad band is observed centred at $\delta_P = 55$ ppm evidencing of the presence of residual phosphinates. At $\delta_P = 33$ ppm a thin peak is detected characteristic of phosphonic acid. The large shouldering going to $\delta_P = 20$ ppm is attributed to phosphonates (phosphorous T^0) or to diphosphonates (phosphorous T^1). Two peaks are also observed at $\delta_P = 2$ and -9 ppm attributed to phosphates and pyrophosphates (Q^1 P). After the 500 °C thermal treatment, the peak attributed to the phosphinates ($\delta_P = 55$ ppm) has disappeared; that phosphonic acid peak centred at $\delta_P = 33$ ppm is still present but with a lower intensity. However, the peak of the pyrophosphates ($\delta_P = -9$ ppm) is enlarged until -30 ppm (polyphosphate Q^3 P) with multiple shoulder at $\delta_P = -2.6$; 2 and 6.5 ppm that can be attributed to orthophosphate species. All phosphorus species seem to be inorganic (Zn) species. However, it is impossible to totally exclude P–O–C bonds which chemical shift would be at $\delta_P = -12$ ppm. On
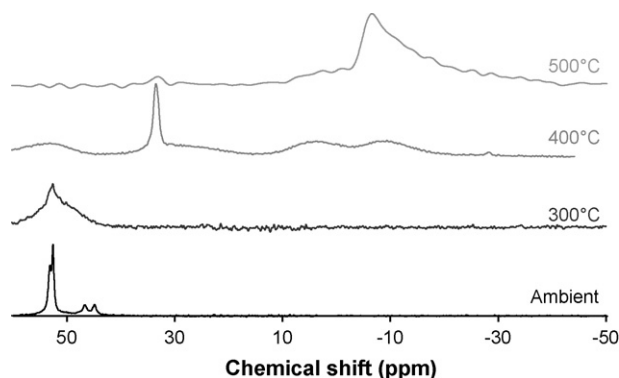

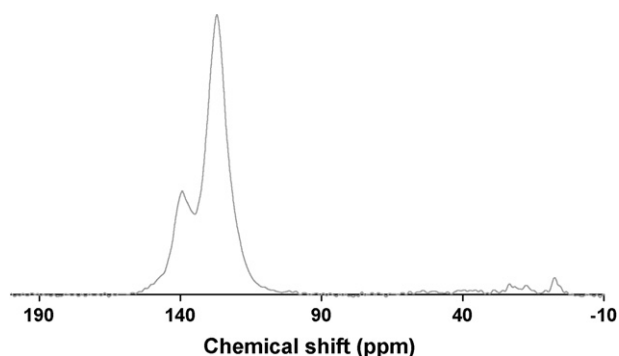**Fig. 24.** DD MAS ^{31}P NMR spectra of the blend PET–OP950 and of the residues of its thermal treatments.

Fig. 25. CP MAS ^{13}C NMR spectrum of the residues of the blend PET–OP950 after TVA.

Fig. 27. ^{13}C NMR spectra of PET–OP950–OMPOSS and of the residues of its thermal treatments.

Fig. 28. CP MAS ^{29}Si NMR spectra of the blend PET–OP950–OMPOSS and of the residues of its thermal treatments.

^{13}C NMR spectra, the signal would be detected at $\delta_C = -130$ ppm if the carbons were aromatics. Phosphonic acid could possibly react with the polymer to form those bonds.

Thus in the presence of PET, OP950 initiates its degradation from 400 °C to form phosphonic acid, phosphonates and phosphates at first that evolve to form pyrophosphates and polyphosphates. The presence of PET seems to prevent the formation of highly branched species in large quantity to the benefit of phosphates and pyrophosphates.

3.5.2. Pyrolysis

The NMR analysis of the residues of the formulation PET–OP950 after the TVA is presented in Fig. 25 for ^{13}C NMR and in Fig. 26 for ^{31}P NMR. The species obtained in the condensed phase are the same than those obtained for the residues of the degradation under air at 400 °C.

On ^{31}P NMR spectra, the peak at $\delta_P = 55$ ppm are attributed to the residual phosphinates, the peak of the phosphonic acid has a high intensity and is centred at $\delta_P = 33$ ppm with a shouldering until 20 ppm due to the phosphonates. Pyrophosphates ($\delta_P = -9$ ppm) remain presents without polyphosphates ($\delta_P < -10$ ppm). Again the presence of P–O–C is not clearly evidenced but cannot be excluded.

On ^{13}C NMR spectra, as for the degradation at 400 and 500 °C under air, the peak attributed to the aromatic carbons of the char at $\delta_C = 130$ ppm is found. The peaks attributed to aliphatic carbons of the C–P and C–C–P bonds are detectable around $\delta_C = 10$ ppm.

3.6. Degradation of PET–OP950–OMPOSS

3.6.1. Thermo-oxidative degradation

In Table 1 are presented the photos of the residues of the formulation PET–OP950–OMPOSS after the different thermal treatment. As for the blend PET–OP950, the structure exhibits
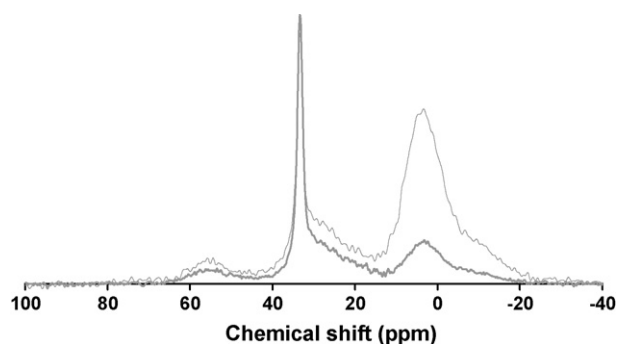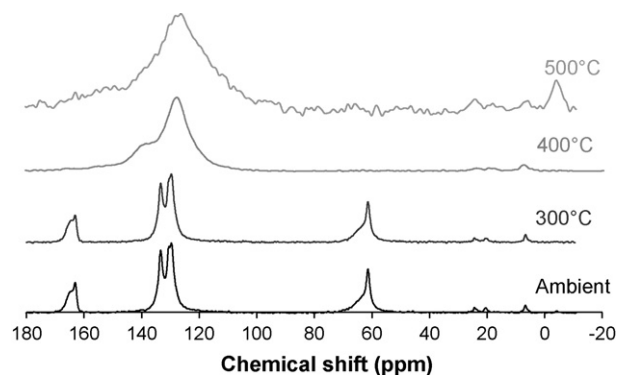
bubbles at 300 and 400 °C. At 500 °C, intumescence is developed and the residue has an expanded carbonaceous structure. The white foamed structure does not appear compared to the blend OP950–OMPOSS. The aspect of the residue is similar to that of the blend PET–OP950.

In Figs. 27–29 are presented the NMR spectra of the blend PET–OP950–OMPOSS and of the residues of its thermal treatment respectively in CP MAS ^{13}C and ^{29}Si NMR and in CP MAS and MAS ^{31}P NMR.

In ^{13}C NMR the same peak than those of the blend PET–OP950 are observed as well as the peak due to the methyl groups of OMPOSS. When the blend is treated at 500 °C, a peak at $\delta_C = -4$ ppm is observed. The intensity of this peak (Si–C bonds) is quite high compared to the other ones but the signal to noise ratio is also low and that leads us to think that, if the detection of those bonds is difficult, then their quantity is lower than the quantity initially

Fig. 26. ^{31}P NMR spectra of the residues of the blend PET–OP950 after TVA (thick curve: CP DD MAS, thin curve: DD MAS).
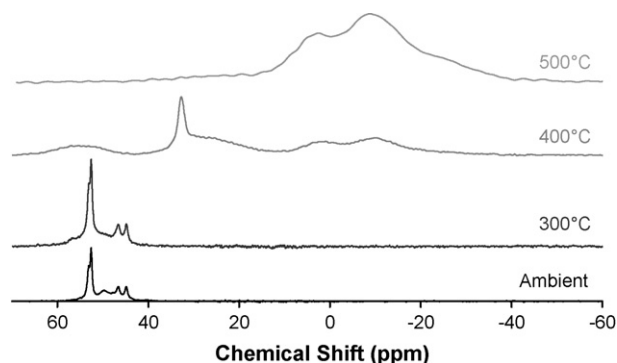

Fig. 29. CP DD MAS (thick curves) and DD MAS (thin curves) ^{31}P NMR spectra of the blend PET–OP950–OMPOSS and of the residues of its thermal treatments.
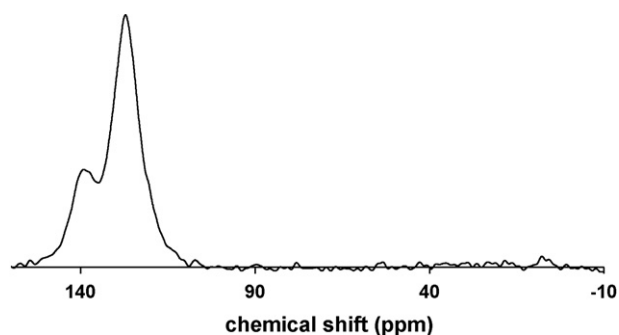
Fig. 30. ^{13}C NMR spectrum of the residues of PET–OP950–OMPOSS after the TVA.

Fig. 31. CP DD MAS (thick curves) and DD MAS (thin curves) ^{31}P NMR spectra of the residues of the blend PET–OP950–OMPOSS after the TVA.

present in the OMPOSS. Alkyl groups of the phosphinates have disappeared. The peak centred at $\delta_C = 130$ ppm is representative of the char exhibiting a condensed aromatic structure.

On ^{29}Si NMR spectra, the same peaks than those observed for OMPOSS alone are observed. The resolution of the spectra is quite low but it can be easily explained because of the low amount of OMPOSS (1 wt.%) in the system. It is still possible to distinguish T^3 silicon at $\delta_{Si} = -66$ ppm as well as the broad band at $\delta_{Si} = -110$ ppm representing Q^4, Q^3 and Q^2 silicon of silica.

On ^{31}P NMR spectra, the species present after the different thermal treatments are similar to those of the blend PET–OP950. After the treatment at 300 °C, the peaks of the phosphinates are not altered. During the 400 °C treatment, the presence of PET leads to the premature degradation of the phosphinate. A broad band centred around $\delta_P = 50$ ppm represents the residual phosphinates in the probably distorted structures giving numerous different P surroundings. A very intense peak at $\delta_P = 30$ ppm is observed with a shoulder going to 20 ppm, relative to the presence of phosphonic acid or diphosphonates and phosphonates. Peaks of phosphates and pyrophosphates are also already observed with a quite high intensity (at $\delta_P = 2$ and $\delta_P = -10$ ppm). After the treatment at 500 °C, the phosphonate band, (broad band of low intensity), is distinguishable at $\delta_P = 25$ ppm. Phosphates are evidenced by a band centred at $\delta_P = 2.8$ ppm and pyrophosphates by a band centred at $\delta_P = -10$ ppm. This last band broadens up to -30 ppm suggesting the presence of polyphosphates. Again the hypothesis of P–O–C bonds is not discarded but the presence of these bonds is not proved. Only the intensity of the phosphates band ($\delta_P = -2.8$ ppm) is different from the one of the blend PET–OP950.

OMPOSS has no influence on the degradation of OP950 when mixed in the PET. The PET leads to a faster degradation of the phosphinates as its degradation begins from 400 °C. Phosphonic acid and phosphonates are formed at this temperature but also phosphates. After the 500 °C thermal treatment, a part of the phosphonates and all the phosphinates are transformed into phosphates, pyrophosphates and polyphosphates.

3.6.2. Pyrolysis

The NMR analysis of the residues of the pyrolysis of the formulation PET–OP950–OMPOSS shows that the same species are formed than during its degradation under air at 400 °C.

On the ^{13}C NMR spectrum (Fig. 30), peaks relative to the char centred at $\delta_C = 130$ ppm can be observed.

On the ^{31}P NMR spectrum (Fig. 31) peaks centred at $\delta_P = 30$, 2, -10, and -20 ppm evidence the presence of phosphonic acid, phosphonates, phosphates, pyrophosphates and polyphosphates. As discussed above, it is possible to assume that the phosphates are formed thanks to the oxygen of the molecules and not with the oxygen from air. That explains the incomplete conversion compared to the oxidative thermal treatment.
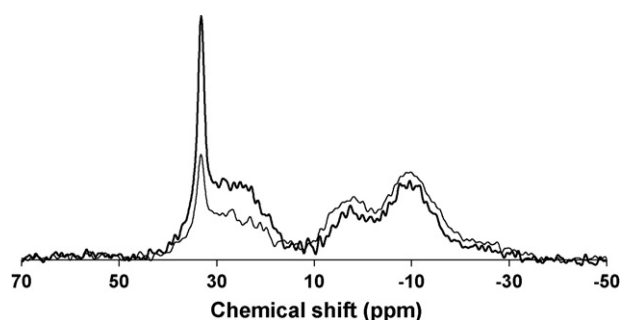
4. Discussion

The analysis of the condensed and gas phase of the OP950 treated at the different temperatures and under different atmospheres (air and nitrogen) lead to identify the different components coming from the degradation. Fig. 32 sums up the different species formed by the additives during their thermal degradation, added or not into the PET. Thus, phosphinates convert into phosphonates, phosphates, pyrophosphates and polyphosphates concurrently with the formation of evolving phosphine.

During the degradation of OMPOSS, multiple rearrangements take place and lead to the formation of siliconorganic species with different oxidation degrees. Those different species can be obtained from the dismutation of OMPOSS and lead to the formation of a silica network.

The combination of OMPOSS and OP950 does not lead to the formation of any species else than those formed by the components taken separately. The two species do not react with each other. In conventional intumescent systems based on ammonium polyphosphate, phosphoric, polyphosphoric or pyrophosphoric acid are usually formed around 300 °C. Those species are very reactive toward other components present in the system and react to form stable species such as titanium, zinc or borophosphate (according to the studied system) [12]. Here, the stables species (zinc pyrophosphate) are formed at 500 °C without going through an intermediate step implicating an acid. That is why, contrary to ammonium polyphosphate-based intumescent systems, no reaction occurs between the phosphorous species and OMPOSS. This phenomenon has also been observed in a study in our Laboratory between aluminium phosphinates and an organo-modified clay: no reaction occurs between the different constituents of the formulation [13].

Under air or under nitrogen, the same species are formed during the degradation of PET–OP950: phosphonates in the beginning of the degradation then phosphates and pyrophosphates. However those species are slightly different from those produced during the degradation of OP950 and particularly phosphonic acid that was not present before. Polyphosphates are present but in a lower quantity. The presence of PET decreases the thermal stability of OP950 that degrades at a lower temperature and leads to the formation of phosphonic acid and phosphates preferentially to branched polyphosphates.

The presence of PET with OP950 leads to a modification in its degradation process. When phosphinates are introduced into the PET, their degradation is accelerated. They form, from 400 °C, phosphonic acid, phosphonates, orthophosphates and pyrophosphates. A broad residual band of the phosphinate is still observed showing that the degradation is incomplete at this temperature. After a treatment at 500 °C, the phosphinate band is no longer detectable. They all converted into orthophosphates, pyrophosphates and polyphosphates to the detriment of phosphonates.
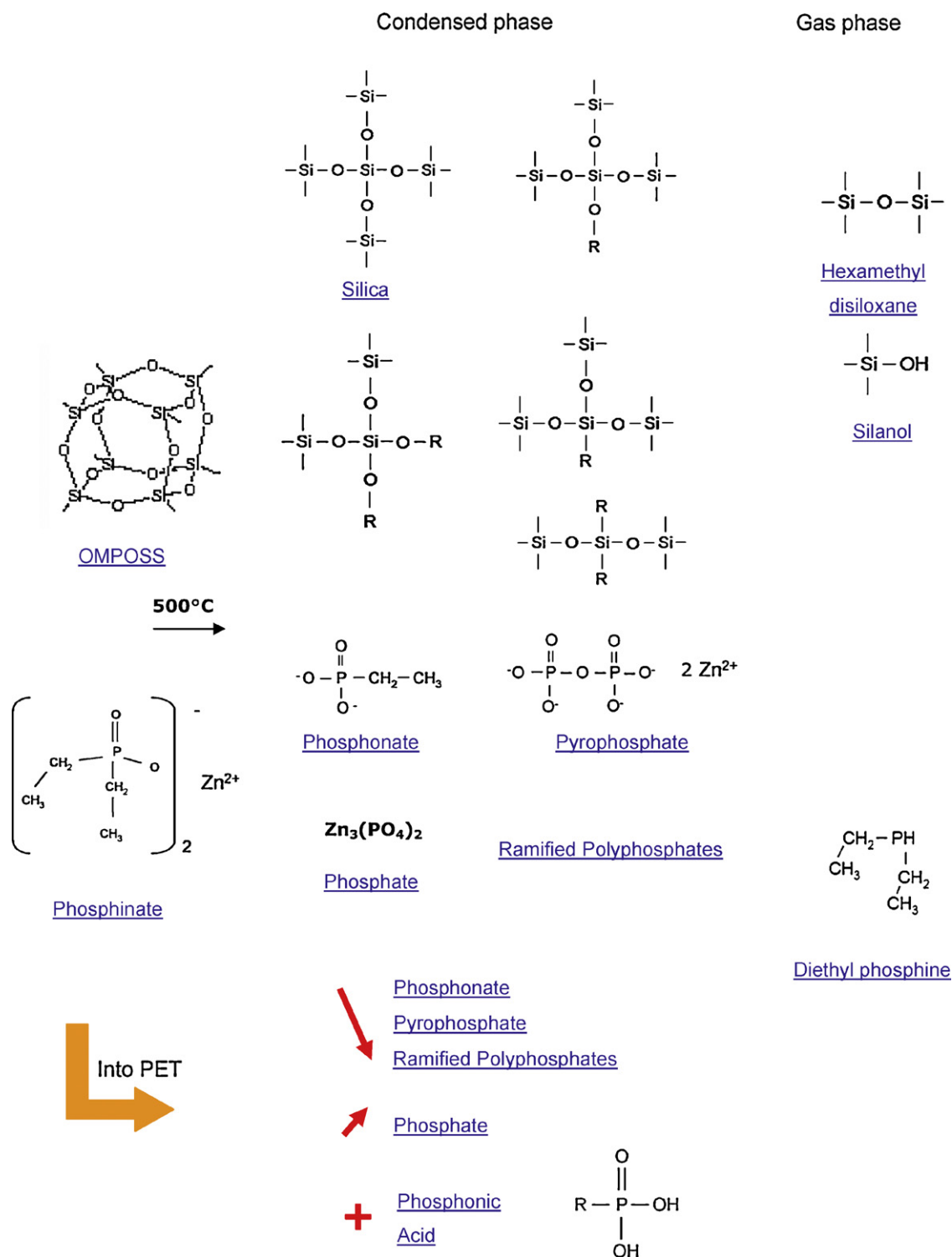
Fig. 32. Species formed during the degradation of the additives.

Under nitrogen, the same phenomenon appears: phosphonic acid is formed whereas it was not during the degradation of OP950 alone. Into the PET, even if orthophosphates and pyrophosphates are present (indicating an oxidation with oxygen via intermolecular reactions with phosphinates (dismutation) and not with air), phosphonates remain certainly because of the lack of oxygen in the system. The products coming from the pyrolysis at 500 °C are the same that in the case of the oxidative degradation at 400 °C.

The degradation of PET catalyses the one of OP950, that, with an earlier degradation, converts more rapidly and totally into phosphonic acid, phosphonates and then into orthophosphates, pyrophosphates, and polyphosphates. The presence of PET prevents the branching of the phosphates into polyphosphates.

The incorporation of OMPOSS in the system PET–OP950 does not modify the species formed. Only an additional silica network is found as for the other system containing OMPOSS.

No chemical interaction appears between OMPOSS and the blend PET–OP950 allowing to explain the improvement of the fire properties. The role of OMPOSS is then probably physical, and linked to their sublimation and/or decomposition into gas products. It is possible to assume that the gases evolved during the degradation of OMPOSS allow a more important swelling of the char and the formation of silica allows its reinforcement.

5. Conclusion

The degradation of OP950 leads to the formation of phosphine in the gas phase and phosphonates, phosphates, pyrophosphates and polyphosphates in the condensed phase. OMPOSS degrades to form mainly silica and other silicone fragments. No chemical interaction occurs between the different components. The different species formed participate to the formation of the char and to its reinforcement assuring a better protection against fire.

In the frame of the fire behaviour of the formulation and the synergy established between the additives, it is possible to assume that the role of OMPOSS is physical in the intumescent system PET–OP950–OMPOSS. The synergy observed between the different components of the formulation is not due to chemical reactions but to a physical effect (sublimation and/or decomposition into gas product of OMPOSS acting as a blowing agent in the intumescent system).

Acknowledgments

References

[1] E. Devaux, M. Rochery, S. Bourbigot, Fire Mater. 26 (2002) 149–154.
[2] S. Bourbigot, M. Le Bras, X. Flambard, M. Rochery, E. Devaux, J. Lichtenhan, Polyhedral oligomeric silsesquioxanes—application to flame retardant textile, in: M. Le Bras, S. Bourbigot, S. Duquesne, C. Jama, C.A. Wilkie (Eds.), Fire Retardancy of Polymers: New Applications of Mineral Fillers, Royal Society of Chemistry, 2005, pp. 189–201.
[3] A. Fina, H.C.L. Abbenhuis, D. Tabuani, G. Camino, Polym. Degrad. Stab. 91 (10) (2006) 2275–2281.
[4] G. Chigwada, P. Jash, D.D. Jiang, C.A. Wilkie, Polym. Degrad. Stab. 89 (2005) 85–100.
[5] A. Vannier, S. Duquesne, S. Bourbigot, A. Castrovinci, G. Camino, R. Delobel, Polym. Degrad. Stab. 93 (2008) 818–826.
[6] http://webbook.nist.gov.
[7] H. Assaaoudi, I.S. Butler, J. Kozinski, F. Bélanger-Gariépy, J. Chem. Crystallogr. 35 (2005).
[8] A. Fina, D. Tabuani, F. Carniato, A. Frache, E. Boccaleri, G. Camino, Thermochim. Acta 440 (2006) 36–42.
[9] Z. Zhang, A.E. Berns, S. Willbold, J. Buitenhuis, J. Colloid Interface Sci. 310 (2007) 446–455.
[10] M. Dzieciol, J. Trzeszczynski, J. Appl. Polym. Sci. 69 (1998) 2377–2381.
[11] M. Dzieciol, J. Trzeszczynski, J. Appl. Polym. Sci. 77 (2000) 1894–1901.
[12] F. Samyn, S. Bourbigot, S. Duquesne, R. Delobel, Thermochim. Acta 456 (2007) 134–144.
[13] F. Samyn, PhD Thesis, Université des Sciences et Technologies de Lille, 2007.